

UNCLASSIFIED

AD 297175

*Reproduced
by the*

ARMED SERVICES TECHNICAL INFORMATION AGENCY
ARLINGTON HALL STATION
ARLINGTON 12, VIRGINIA



UNCLASSIFIED

NOTICE: When government or other drawings, specifications or other data are used for any purpose other than in connection with a definitely related government procurement operation, the U. S. Government thereby incurs no responsibility, nor any obligation whatsoever; and the fact that the Government may have formulated, furnished, or in any way supplied the said drawings, specifications, or other data is not to be regarded by implication or otherwise as in any manner licensing the holder or any other person or corporation, or conveying any rights or permission to manufacture, use or sell any patented invention that may in any way be related thereto.

65-2-15

28 December 1962



USCEC REPORT 65-35

COPY 9

297175

UNIVERSITY OF SOUTHERN CALIFORNIA

SCHOOL OF ENGINEERING

DESCRIPTION OF AN EXPERIMENTAL INVESTIGATION OF THE
EFFECT OF BOUNDARY LAYER BLEED ON SHOCK
WAVE-BOUNDARY LAYER INTERACTION

John B. Wainwright

*Qualified requesters may
obtain copies of this
report from ASTIA.*

AERODYNAMIC TEST LABORATORY
U. S. NAVAL MISSILE CENTER
POINT MUGU, CALIFORNIA

297175

USCC
Engineering Center

AERODYNAMIC TEST LABORATORY, NMC

OPERATED BY THE UNIVERSITY OF SOUTHERN CALIFORNIA

Engineering Center

28 December 1962

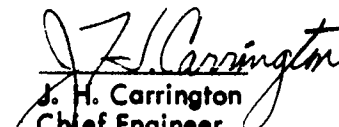
USCEC REPORT 65-35

DESCRIPTION OF AN EXPERIMENTAL INVESTIGATION OF THE
EFFECTS OF BOUNDARY LAYER BLEED ON SHOCK
WAVE-BOUNDARY LAYER INTERACTION

By:

John B. Wainwright

Approved By:


J. H. Carrington
Chief Engineer
USCEC - ATL

CONTENTS

	PAGE
BACKGROUND	1
DESCRIPTION OF TESTS	2
TEST PROGRAM OUTLINE	4
COMMENTS	5
Three-Dimensional Effects	5
Effects of Porous Plate Hole Size	7
REFERENCES	8

LIST OF FIGURES

Figure 1,	Flat Plate and Shock Generator Mounted in Model Support Section	9
Figure 2,	Schematic of Test Apparatus	10
Figure 3,	Plate Dimensions	11
Figure 4,	Solid-20% Plate	11
Figure 5,	Solid-20%-Solid Plate	11
Figure 6,	Slotted Plates	11
Figure 7,	Schematic of Porous Plate Static Pressure Orifice Locations	12
Figure 8,	Schematic of Generator Plate Static Pressure Orifice Locations	13
Figure 9,	Schematic of Bleed Chamber Static Pressure Orifice Locations	13
Figure 10,	Static Pressure Distribution on the Solid and the Solid-20%-Solid Plates	14
Figure 11,	Paint Flow Photograph	15
Figure 12,	Flow Diagram for Figure 11	15
Figure 13,	Region Where the Flow was Influenced by the Edges of the Wedge	16
Figure 14,	Percent Change in Total Pressure as the Pitot Probe is Moved Horizontally Over a Hole in the 50%-Porous Plate	16
Figure 15,	Pressure Ratio Across Shock Impingement to Produce Separation vs Bleed Flow	17

BACKGROUND

Problem Assignment 1-34-13 (Formerly designated TED NMC AD 3066 (ATD)) was assigned to the Aerodynamic Test Laboratory (ATL)* by Reference 1 in April 1958 in support of a joint program undertaken by the Bureau of Naval Weapons and the Columbus Division of North American Aviation, Inc. (NAA) to investigate the effects of suction on shock wave-boundary layer interaction characteristics, with the view of establishing engineering design criteria for supersonic air-induction systems. The division of effort, as specified in Reference 2, gave NAA the responsibility for the design and direction of the experiments, the furnishing of models, and the analysis and reporting of the test results. The Bureau of Weapons provided the facilities and services of the ATL for the experiments.

The tests were made intermittently during the period 4 April 1959 - 29 July 1959 and consumed a total of 211.1 occupancy hours in the ATL wind tunnels. Data from all measurements were reduced at the ATL and sent to NAA by a series of informal letters. NAA has issued a final report (Reference 3) in which the data is correlated empirically and with respect to simple analytical models of the flow. A sample problem is also presented in which the results are applied to the design of a supersonic inlet and ducts.

The purpose of the present report is to describe and to offer comment on the experiments and the experimental technique. It is not considered useful to extend or to duplicate the kind of analysis of the data which has already been presented in Reference 3.

* The ATL was established by the Bureau of Naval Weapons to assist Naval contractors in airplane and missile development projects at the U. S. Naval Missile Center, Point Mugu, California. Since completion of the facilities in 1951, the ATL has been operated by personnel of the University of Southern California Engineering Center.

DESCRIPTION OF TESTS

All tests were conducted in the ATL Mach number 2.58, 17" x 21" fixed-geometry nozzle and Mach number 3.0 - 3.5, 22" x 21" variable-geometry nozzle. Both nozzles were driven by the same continuous air supply at a stagnation temperature of 110° - 125°F and stagnation pressures ranging from 3.0 to 3.8 atmospheres. Humidity of the test air was maintained below .05 percent in order to prevent measurable effects from condensation.

The special apparatus used to model the boundary layer shock wave was furnished by NAA and is illustrated in Figures 1 and 2. The boundary layers were developed on the upper surface of a 6° wedge of trapezoidal plan form, supported in the wind tunnel test section on a pedestal mounting. The wedge had a leading-edge span and over-all length of 16.5 inches, and a 20° tip-rake angle. The first 3.5 inches of the wedge surface was solid, and this was followed by interchangeable surfaces of various porosities and distributions of porosity. In order to assure experimental two-dimensionality, all measurements were made within a one-inch strip running down the center of the wedge surface. Metered bleed flows were thus drawn from compartments one inch in width, ducted to the outside of the tunnel through standard ASME orifice metering runs controlled with a sonic throttle valve, and then injected back into the tunnel near the entrance to the tunnel's diffuser. Similarly, static pressures and pitot pressure profile were measured within the bounds of the one-inch strip. Bleed flow rates in the compartments outboard of the center strip were not metered but were controlled with remotely-operated valves so that the pressures within adjacent compartments could be matched.

The bleed compartments were also partitioned by a divider strip across the flow direction at the theoretical line of shock impingement in order to support the pressure gradient induced by the shock and to prevent recirculation in the bleed chamber.

The entire wedge could be inclined with respect to the nozzle flow in order to provide a pressure difference sufficient to pump the bleed chambers. Inclination angles suitable for all anticipated configurations and test conditions were fixed early in the test and thereafter held constant. These established the following test conditions associated with the flow over the wedge surface upstream of shock impingement:

Nozzle Mach No.	Wedge Mach No.	Wedge Reynolds No. (Per Inch)
2.58	2.3	$.79 \times 10^6$
3.0 - 3.5	3.0	$.72 \times 10^6$

Shock waves were impinged on the wedge surface from a shock generator plate. Its inclination relative to the wedge surface and distance from the wedge surface could be varied, such that pressure rise ratios up to 5.0 could be established on the plate at the bleed compartment divider station (13.0 inches from the wedge's leading edge).

The various porous plate configurations investigated in the test series are illustrated in Figures 3 to 6. All plates were 0.062 inches thick and had 0.06-inch diameter holes. Figure 3 is applicable to the completely uniform 20% and 50%-porosity plates with holes normal to the surface, 50% plates with holes inclined 30° and 60° to the normal, and a 50% plate with 0.06" x 0.12" oval holes. Figures 4 and 5 show combinations of solid and 20%-porosity plates, and Figure 6 shows two simple bleed slot configurations that were added to the program during the second series of tests.

The sites of static pressure measurements on the plate surfaces and in the bleed chambers are indicated in Figures 7, 8 and 9.

Pitot pressure profiles were measured with a single probe, remotely controlled for both vertical and longitudinal displacement. Vertical displacements were measured to a

precision of .004 inches on an engraved scale which was incorporated in the control mechanism. Indexing was accomplished by observing the break of electrical contact between the probe tip and the plate surface. Dimensions of the probe tip were .0015 inches by .008 inches.

TEST PROGRAM OUTLINE

The test program had three principal divisions. In the first (Runs 1-199), pitot pressure profiles of the boundary layer were measured at locations considered to be upstream, within and downstream of the shock wave-boundary layer interaction region. Physically these locations were 0.6 inches upstream of the theoretical shock impingement station and 0.8 and 2.6 inches downstream. These measurements were made over the solid, 20%- and 50%-porosity plates at nominal Mach numbers 2.3 and 3.0, and with the shock generator angle fixed at about 10° with respect to the plate. The effects of from five to ten different combinations of forward and aft bleed were investigated for each plate.

In the second series of tests (Runs 200 to 253), a detailed investigation of the variation in pitot pressure profile within the interaction region was made over the 20%-porosity plate at Mach number 2.3 at a relatively fixed shock strength (the shock generator angle ranged from 11.5 to 13.8 degrees). Six combinations of bleed were investigated in this phase.

The final phase of the test (Runs 312 to 494) attempted to determine minimum suction rates for the prevention of boundary layer separation at various shock strengths for five different plate configurations. These were 1) the full 50%-porosity plate with oval holes, 2) the 20% plate, 3) the solid plate up to the divider followed by 20% porosity aft of the divider, and 4) and 5) the 2-inch 20%-porosity strip with leading edge $3/4$ inch

upstream of the divider and two bleed slots, 0.3" and 0.6" wide, located just downstream of the divider. The criterion used to identify separation was the existence of an inflection point in the distribution of static pressure in the interaction region. All tests in this final phase were made at Mach number 2.3.

COMMENTS

Three-Dimensional Effects

As indicated earlier in this report, the general objective of the investigation was to develop a body of experimental data on the effects of suction on the shock wave-boundary layer interaction which would be applicable to specific engineering problems, such as the design of supersonic air inlets. Data derived from a plane shock impinging on a two-dimensional boundary layer were considered to have the widest range of applications, and this requirement led to the development of the trapezoidal-shaped test plate with the one-inch-wide center strip over which all measurements were made. Bleed rate controls were provided for the areas adjacent to the strip in order to assure uniform boundary layer bleed rates along lines normal to the flow, and the sides of the plate were raked at an angle such that they could not influence the center strip at the designed free-stream test Mach numbers. The shock generator was given sufficient span to assure the impingement of a uniform plane shock along the entire span of the boundary layer plate, and sufficient chord length was provided to place the influence of the trailing edge downstream of all measurement stations.

Thus, in principle, measurements within the center strip would characterize two-dimensional flow. In practice, however, significant departures from two-dimensionality were encountered during the test series. The most obvious manifestation of this was the fact that the two-dimensional pressure rise associated with shock impingement was never

achieved. This is illustrated in Figure 10, which shows the pressure distribution induced on the plate from the shock generator inclined at an angle of 16.3° . The two-dimensional pressure rise for such conditions would be about 5.5, whereas the measured values never reached 5.0. This is accounted for by the fact that the raked edge on the side of the boundary layer plate became increasingly subsonic as the strength of the shock increased and reduced the Mach number downstream of the shock. The resultant "spillage" of high-pressure air around the sides of the plate induces spanwise flow gradients over the plate and reduces the pressure at the center strip. These effects are also manifested by the apparent curvature of the line of shock impingement, which was observed for a few cases on a solid plate painted with viscous paint to aid flow visualization (See Figures 11 and 12). In these cases the boundary layer near the sides was thinned by bleed along the spanwise pressure gradient. The corresponding reduction in upstream propagation of the shock-induced separation line gives the appearance of a shock impingement line that curves back in a downstream direction as the sides of the plate are approached.

Figure 10 also illustrates the influence of boundary layer bleed on pressure rise. It is seen that without bleed the interaction region is relatively large, and the region of pressure rise is spread out and merges into the increasing effects of side spillage further on down stream. With bleed, steeper pressure gradients are supported and higher peak pressure rise ratios are achieved.

It is not considered that these effects seriously compromise the general objectives of the test, since correlations can be made with the measured pressure rise rather than with the theoretical two-dimensional value. However, careful judgment must be exercised in a determination of the point at which the measured pressures are not influenced by the interaction of the pressure rise with the boundary layer.

It should also be noted that at Mach number 2.3 the entire side edge of the plate was subsonic, and thus spanwise pressure gradients were induced over the plate in the

regions bounded by the edges and the Mach number 2.3 Mach lines; see Figure 13. While there was no attempt made to measure the effects of these gradients on the boundary layer over the center of the plate, their influence is considered negligible in view of the distance from the Mach line to the plate center relative to the boundary layer thickness.

Effects of Porous Plate Hole Size

It became evident early in the attempts to measure boundary layer profiles with suction that the lateral position of the pitot pressure probe relative to a hole on the porous plate made a significant difference in the measured pressures.

Some typical variations are illustrated in Figure 14 where it is seen that, for moderate suction rates, a 10% variation in measured pitot pressure exists at a level of half the boundary layer thickness between points separated by only the distance of a hole diameter. This is not surprising, since most suction rates were large compared with the rates at which a turbulent boundary layer could remove mass flow from the free stream through viscous shearing forces on a smooth plate (10 to 15 times larger for conditions downstream of shock impingement). As a consequence, the thickness of the boundary layers with bleed were on the same order as the size of the bleed holes, and the suction-induced gradients normal to the plate of normal velocity, pitot pressure, pressure and temperature would be expected to extend into the boundary layer.

During the test, care was taken to locate the pitot probe over a solid portion of the porous plates between the holes. This procedure, while giving the measurements an internal consistency, does not alter the fact that all measured pitot profiles were peculiar to the site of the measurements relative to the holes in the plate and therefore cannot, in principle, be reduced to relationships independent of hole configuration and size.

It is considered, therefore, that the gross results from the test program such as characteristic shock wave-boundary layer interaction lengths, boundary layer thickness downstream of the interaction, etc, can be applied to engineering problems such as the design of supersonic air-induction systems, provided the general features of the porous plate configurations are duplicated with the same bleed rates relative to the local free-stream mass flow.

These bleed rates were so large that a run of a few boundary layer thicknesses in length is sufficient to establish the new equilibrium thickness with suction. Therefore there is no benefit from a long run of bleed before shock impingement. The two-inch run of the 20%-porous plate and the 0.3" and 0.6" bleed slots were, as a matter of fact, even more effective in supporting large pressure gradients than the long runs of porous plate and, of course, much more economical with bleed air. This is illustrated in Figure 15, where the pressure ratio associated with incipient separation is plotted vs. total bleed flow per unit width of porous plate.

It should be noted that these performance levels involve carefully locating the shock impingement line at the divider in the case of the porous plate, or in the slot for bleed-slot configurations. Thus if the design involves a variation in shock location, additional bleed locations or dividers would have to be provided.

REFERENCES

1. BuAer Ltr. Aer-AD-312/329 of 27 March 1959.
2. NAA Ltr. 58 CL 5957 (Confidential) of 23 June 1958.
3. Simon, W. E., "An Experimental Investigation and Correlation of the Effects of Boundary Layer Bleed on Shock Wave-Turbulent Boundary Layer Interaction", NAA Report NA 60H-401 (Confidential), 21 July 1960.

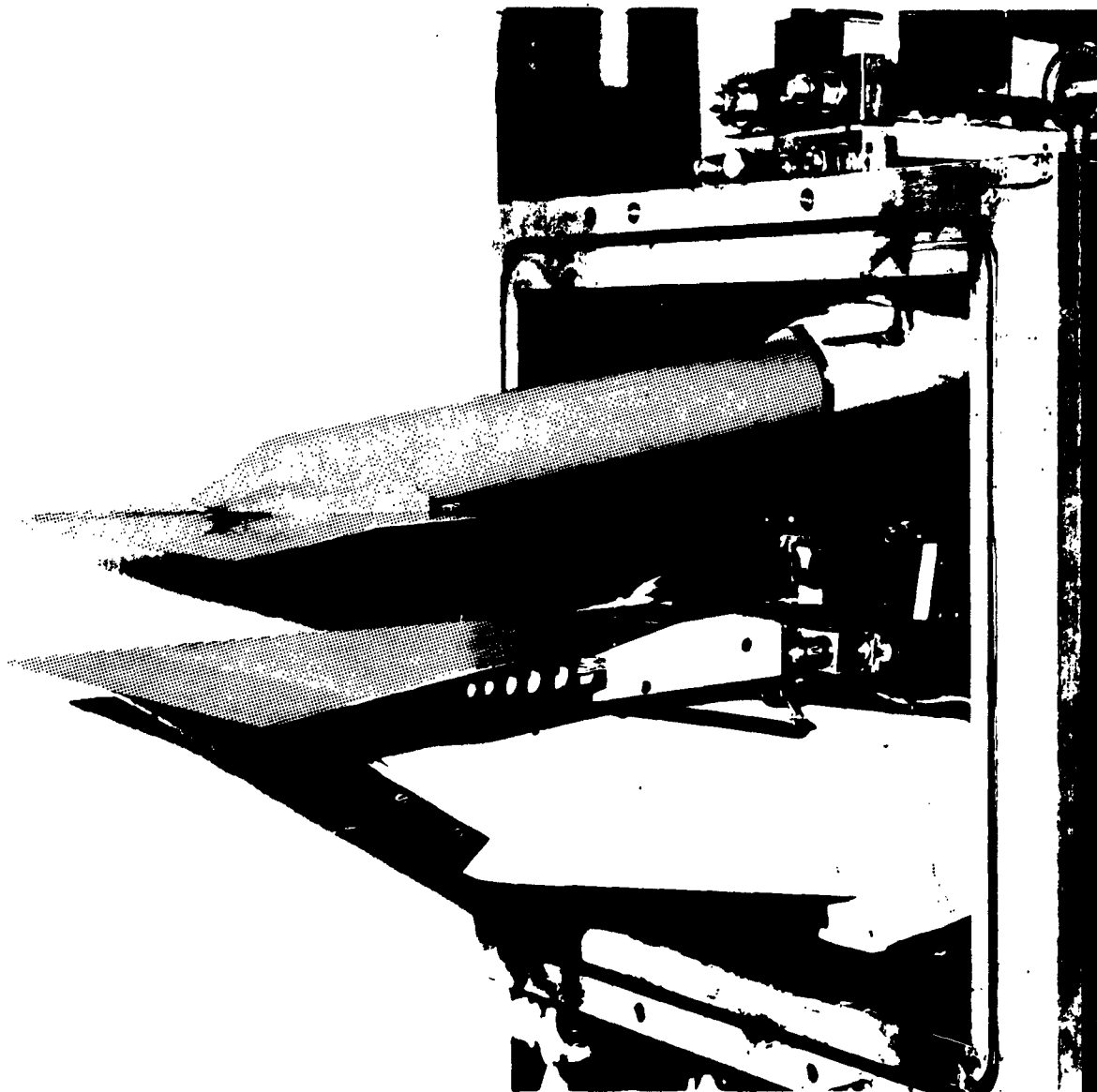


FIGURE 1, FLAT PLATE AND SHOCK GENERATOR
MOUNTED IN MODEL SUPPORT SECTION

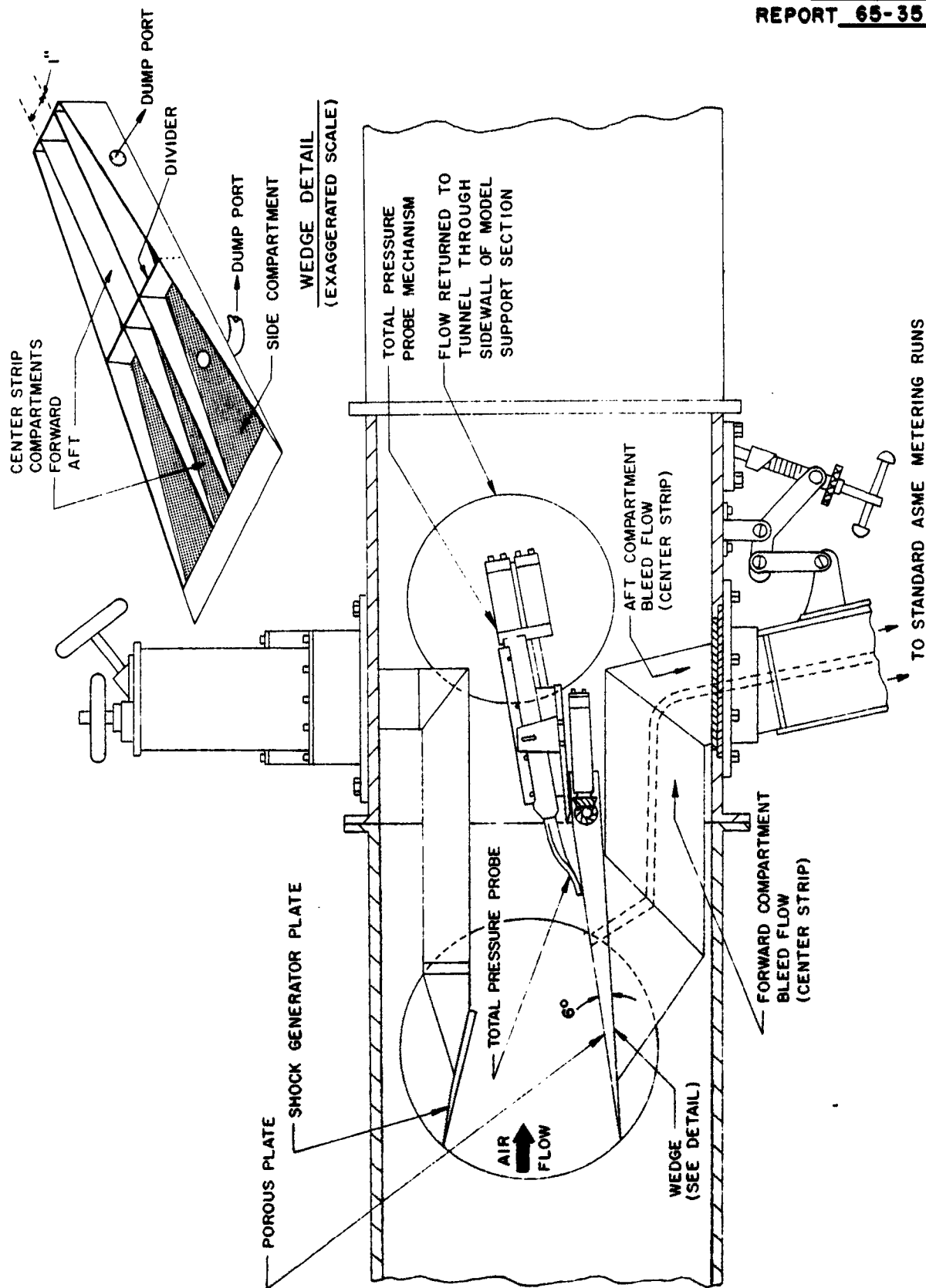


FIG. 2, SCHEMATIC OF TEST APPARATUS

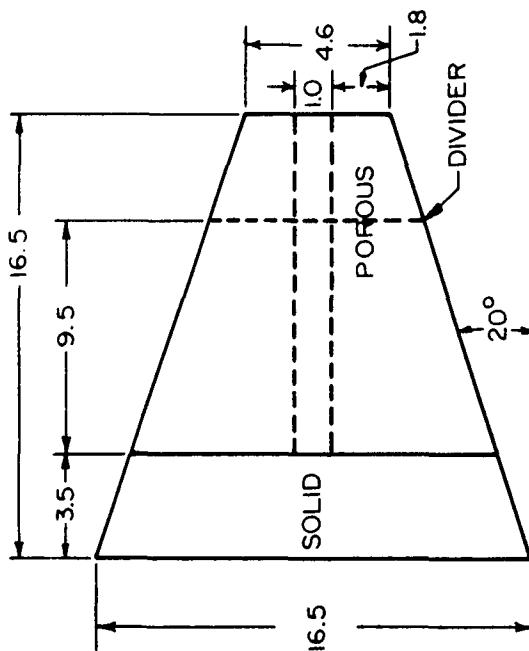


FIG. 3, PLATE DIMENSIONS (IN.)

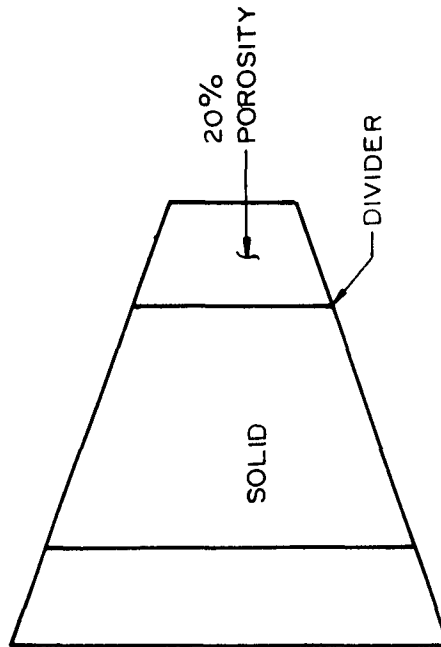


FIG. 4, SOLID-20% PLATE

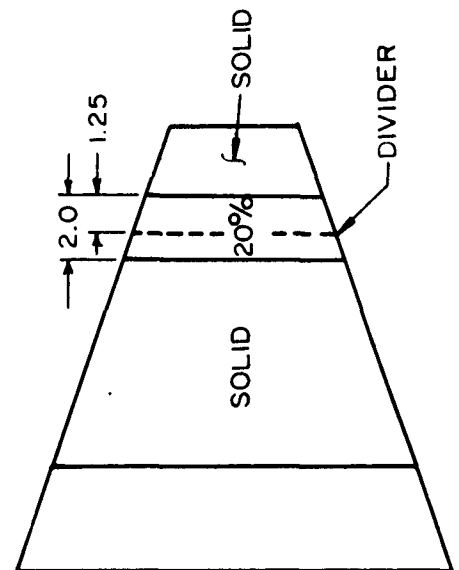


FIG. 5, SOLID-20%-SOLID PLATE

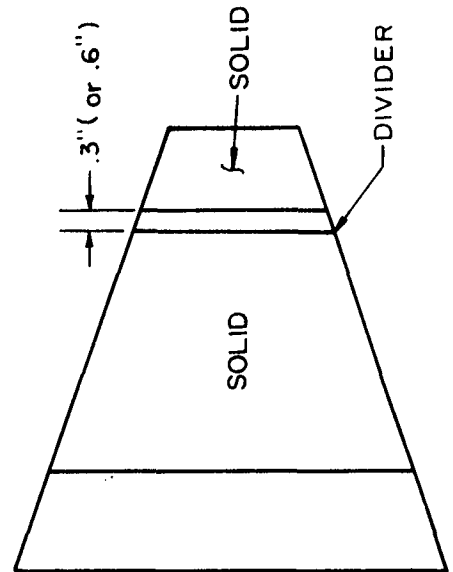


FIG. 6, .3" (.6") SLOTTED PLATE

AERODYNAMIC TEST LABORATORY, NMC

OPERATED BY THE UNIVERSITY OF SOUTHERN CALIFORNIA

Engineering Center

PAGE 12

REPORT 65-35

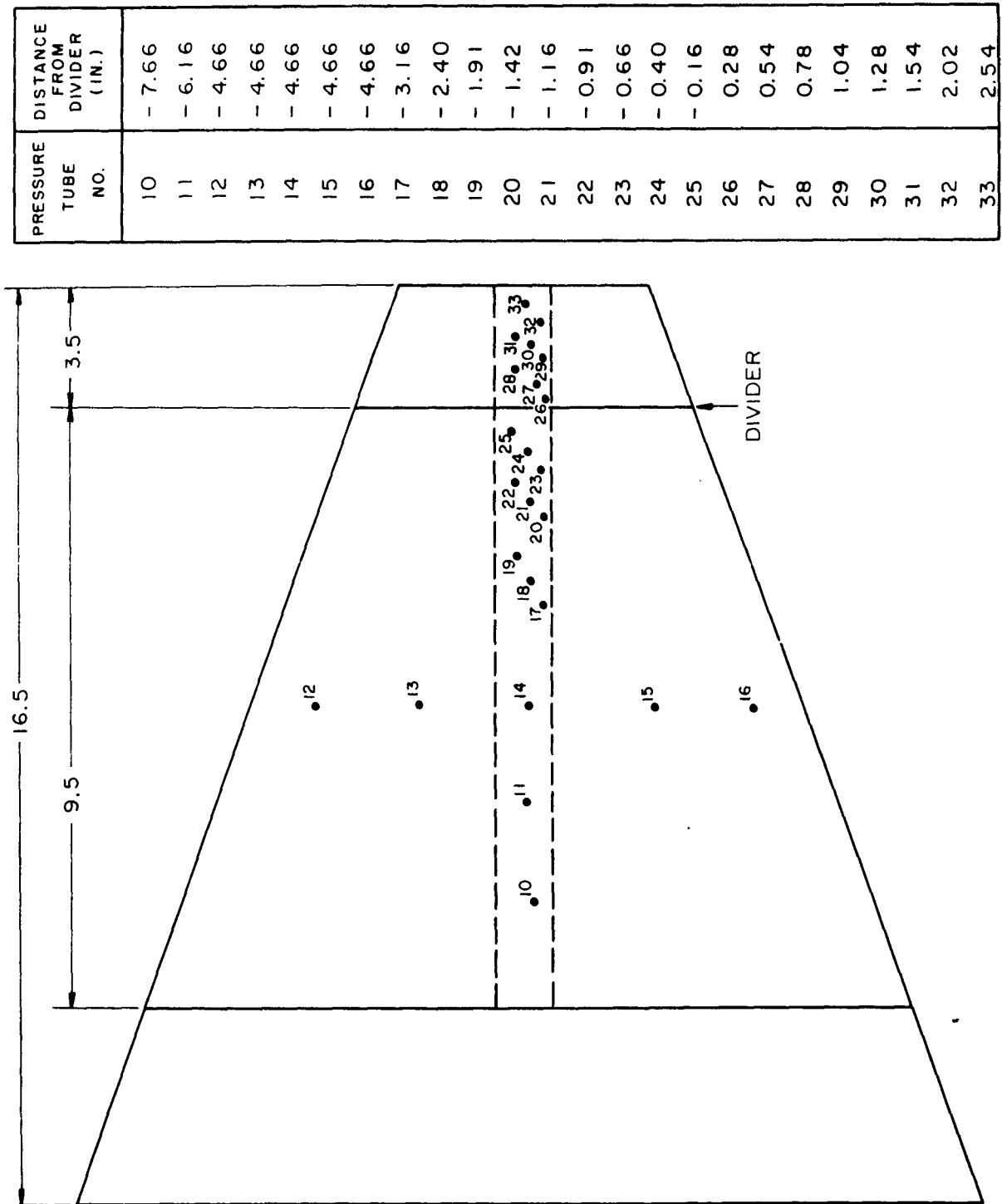


FIG. 7, SCHEMATIC OF POROUS PLATE STATIC PRESSURE ORIFICE LOCATIONS

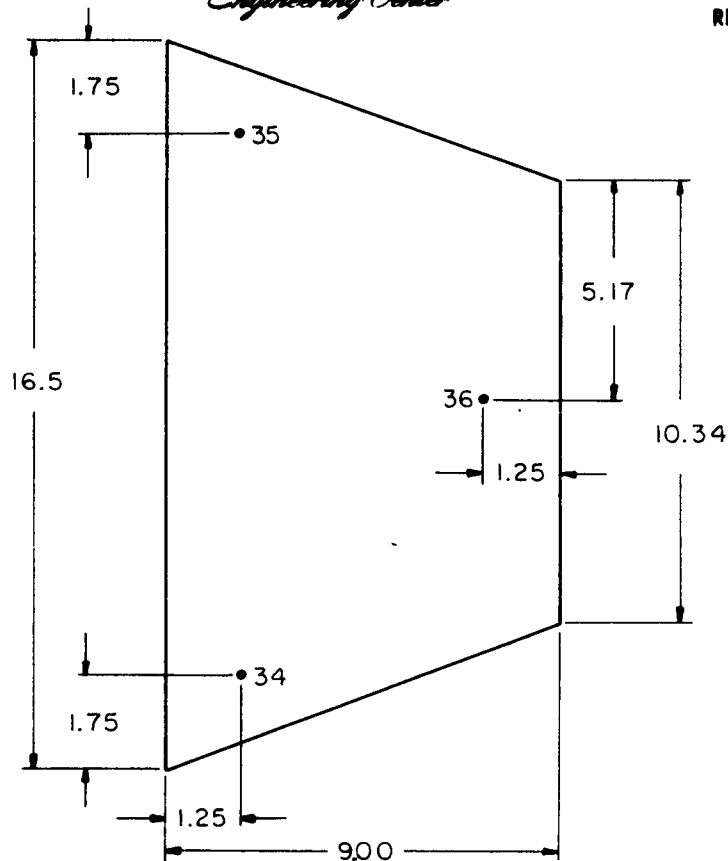


FIG. 8, SCHEMATIC OF GENERATOR PLATE STATIC PRESSURE LOCATIONS

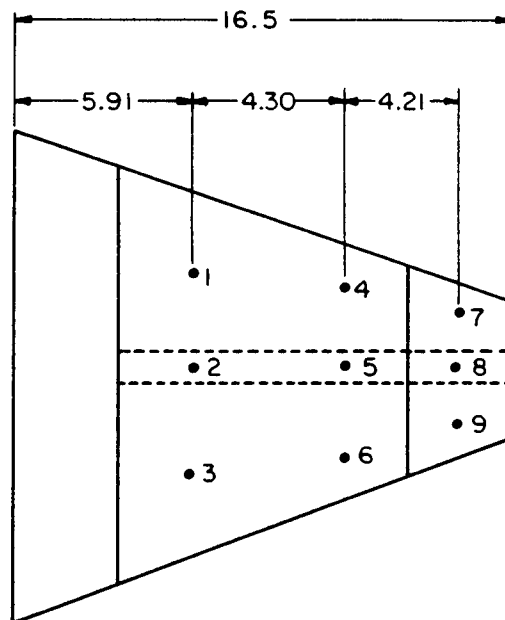


FIG. 9, SCHEMATIC OF BLEED CHAMBER STATIC PRESSURE LOCATIONS

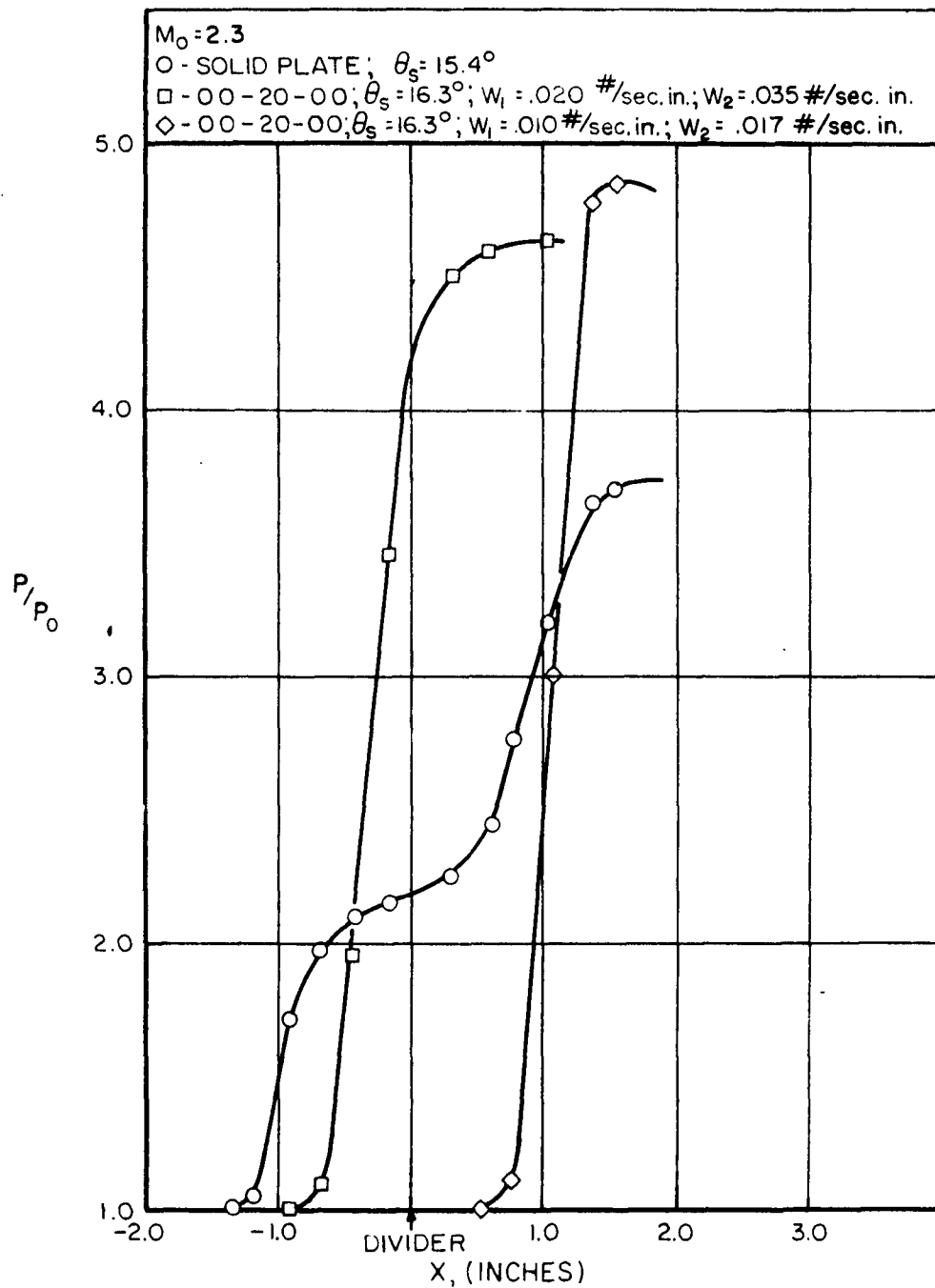


FIG.10, STATIC PRESSURE DISTRIBUTION ON THE SOLID AND THE SOLID-20%-SOLID PLATES



FIGURE 11, PAINT FLOW PHOTOGRAPH

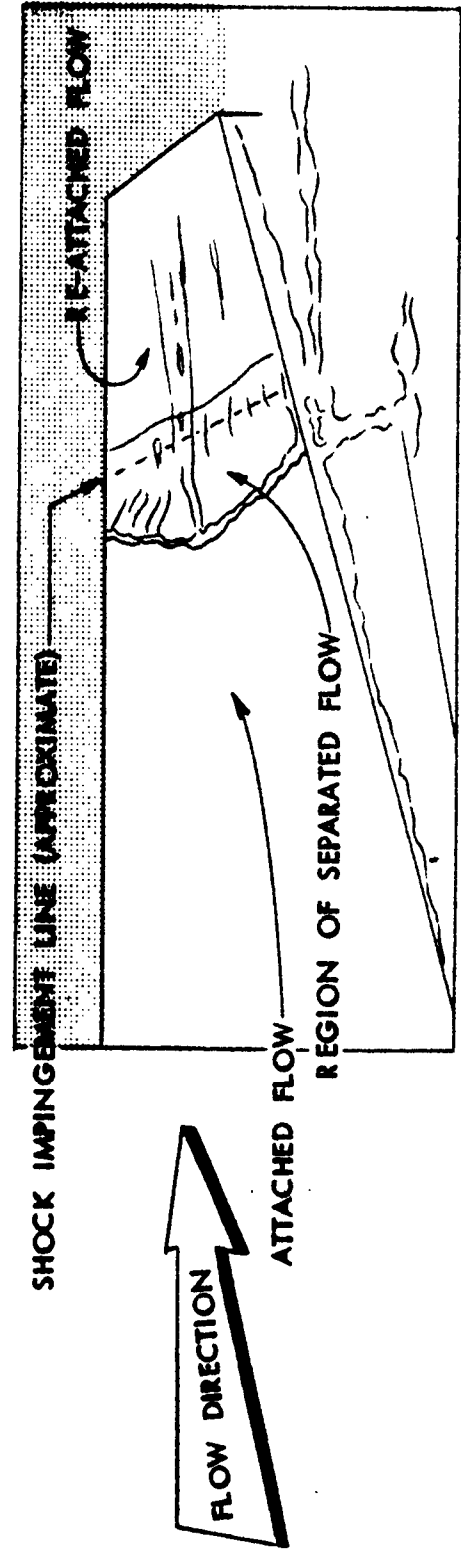


FIGURE 12, FLOW DIAGRAM FOR FIGURE 11

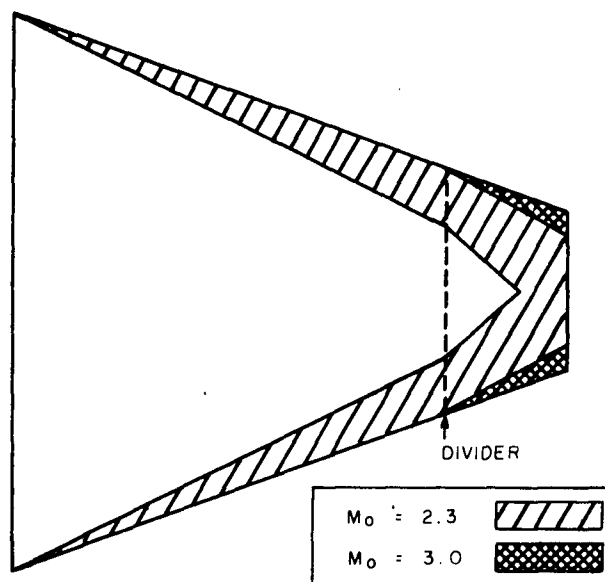


FIG. 13, REGION WHERE THE FLOW WAS INFLUENCED BY THE EDGES OF THE WEDGE. (ASSUMED $\theta_s = 10^\circ$)

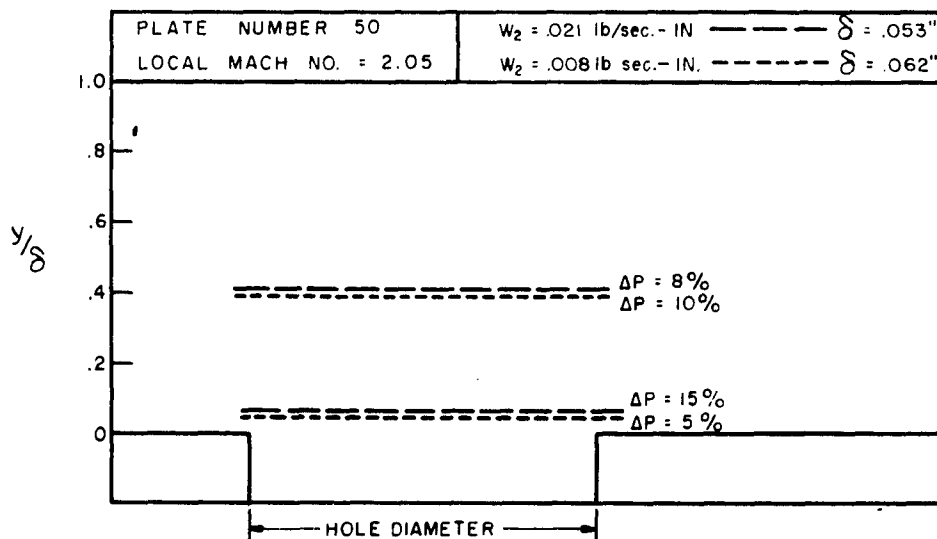
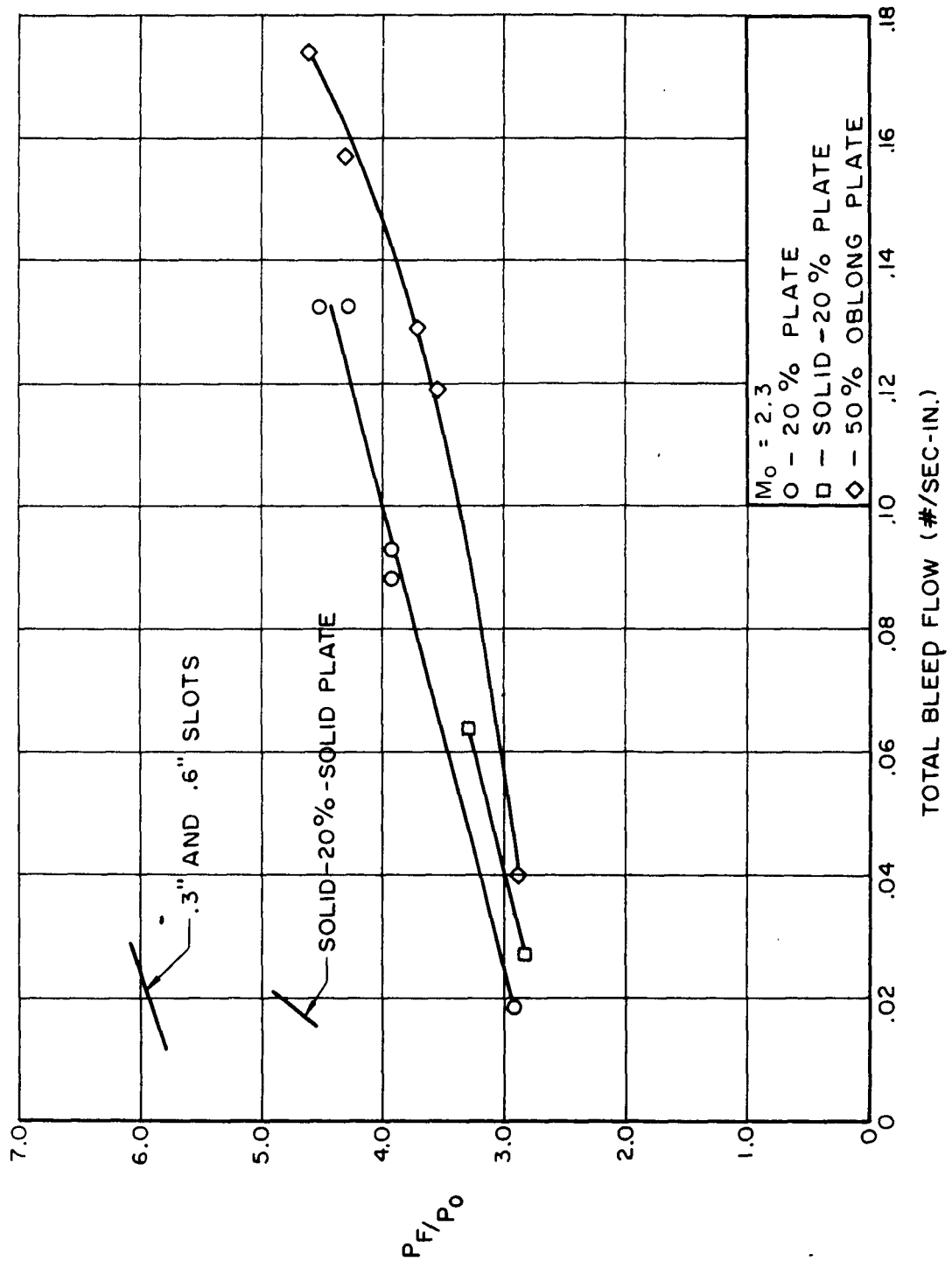


FIG. 14, PERCENT CHANGE IN TOTAL PRESSURE AS THE PITOT PROBE IS MOVED HORIZONTALLY OVER A HOLE IN THE 50%-POROUS PLATE.

FIG. 15, PRESSURE RATIO ACROSS SHOCK IMPINGEMENT TO PRODUCE SEPARATION
VS BLEED FLOW